THE OFFICIAL MAGAZINE OF THE OCEANOGRAPHY SOCIETY

Oceanography

CITATION

Matveeva, T., A.S. Savvichev, A. Semenova, E. Logvina, A.N. Kolesnik, and A.A. Bosin. 2015. Source, origin, and spatial distribution of shallow sediment methane in the Chukchi Sea. *Oceanography* 28(3):202–217, http://dx.doi.org/10.5670/oceanog.2015.66.

DOI

http://dx.doi.org/10.5670/oceanog.2015.66

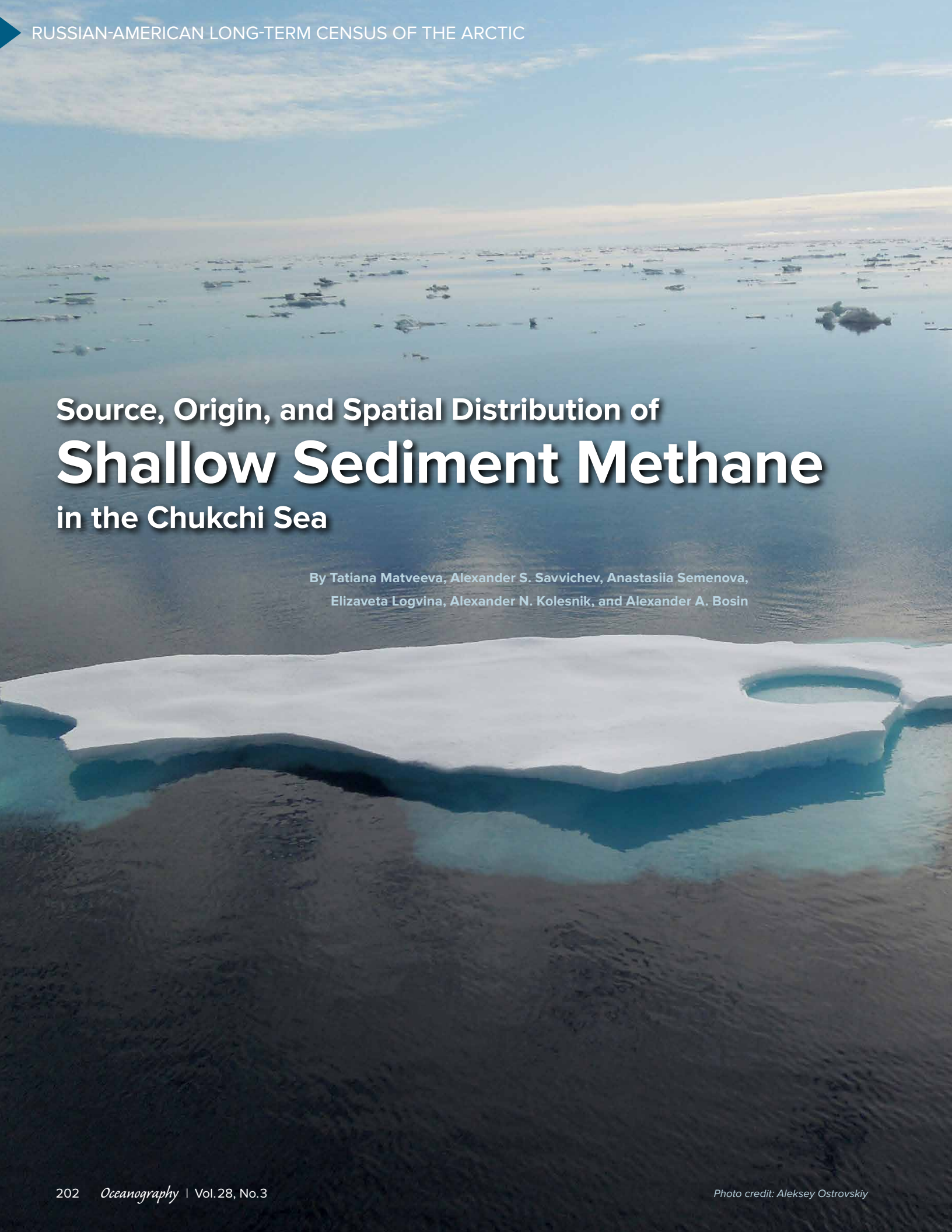

Source, Origin, and Spatial Distribution of Shallow Sediment Methane in the Chukchi Sea

By Tatiana Matveeva, Alexander S. Savvichev, Anastasiia Semenova, Elizaveta Logvina, Alexander N. Kolesnik, and Alexander A. Bosin

Photo credit: Aleksey Ostrovskiy

ABSTRACT. It is essential to study methane in the Arctic environment in order to understand the potential for large-scale greenhouse gas emissions that may result from melting of relict seafloor permafrost due to ocean warming. Very few data on the sources of methane in the Chukchi Sea were available prior to initiation of the Russian-American Long-term Census of the Arctic (RUSALCA) program in 2004. This article documents for the first time the spatial variation of methane concentrations in the sediment and water column in a significant region of the Pacific Arctic and the influence of methane turnover and net transport from organic-rich environments within the western Chukchi Sea. The study combines historical observations, new data obtained during the RUSALCA collaborative program, and modeling results to provide insights into the contemporary methane dynamics of the western Chukchi Sea. We compare methane evolution at two sites with distinct geological settings, depositional patterns, and methane sources: (1) the deeper, fault-bounded Herald Canyon (northern site) where methane flux is controlled by both northward CH_4 transport via ocean currents and diffusive influx of thermogenic methane (formed under high-temperature conditions) from source rocks at depth in the canyon's seafloor, and (2) the shallow Chukchi shelf (southern site), where sulfate reduction and anaerobic methane oxidation play a significant role in biogenic methane production and its flux within and from the sediments into the water column. Diffusive methane fluxes at the sediment-water interface within the southern and northern sites were estimated to be 14.5 μmol dm^{-2} day^{-1} and 0.7 nmol dm^{-2} day^{-1}, respectively. In addition, we suggest that biogenic methane emanating from the organic-rich southern region is transported northward by the Anadyr Current, leading to a mix of both biogenic and thermogenic methane in Herald Canyon surface waters. Study results indicate that the South Chukchi Basin is an important source of atmospheric CH_4. Further work is required to accurately quantify this flux.

INTRODUCTION

Thawing of terrestrial and relict seafloor permafrost and the resultant release of methane into the hydrosphere and atmosphere has the potential to be one of the most significant contributions to increased warming of the Arctic environment. Furthermore, biogenic and thermogenic processes associated with shallow seafloor fluid flow affect benthic ecology (Judd, 2003; Judd and Hovland, 2007). To date, the best-studied shallow seafloor release of methane was documented in the Laptev, East Siberian, and South Kara Seas, where large quantities of this powerful greenhouse gas are reaching the Arctic atmosphere (Shakhova et al., 2010; Portnov et al., 2013). Whether this flux results from warming of seafloor permafrost in these regions or has been a constant flow since the end of the last ice age requires additional long-term observations (Isaksen et al., 2011).

Methane-related processes in the shallow Chukchi shelf, east of the East Siberian Sea between Russia and the United States, are thought to be sensitive to fluctuating conditions in the water column such as increases in Bering Strait throughflow, temperature, and bottom-water hypoxia. Ocean water circulation is an important sediment transport mechanism in this marginal sea. Waters are channeled through Bering Strait and exit into the Arctic Ocean through Herald and Barrow Canyons on the western and eastern sides of the Chukchi Sea, respectively (Viscosi-Shirley et al., 2003).

Both concentrated and dispersed seepages of hydrocarbon gases from shallow sedimentary layers are common phenomena, resulting either from in situ formation of gases (mainly methane) by bacterial decomposition of organic matter within rapidly accumulating upper marine sediments, or from an upward migration of

gases formed at greater depths (Claypool and Kaplan, 1974; Reeburgh, 1996).

The occurrence of methane in marine sediments of shallow seas is closely associated with organic matter decomposition and is governed by various biological and geochemical processes (Claypool and Kaplan, 1974; Davis, 1992; Reeburgh, 1996). Bacterial methane production in sediments is mediated by a complex microbial community and ultimately controlled by the flux of reactive organic matter and by seasonal temperature variations that strongly influence both the rate and the pathways of methane production (Zeikus and Winfrey, 1976; Schulz and Conrad, 1996; Schulz et al., 1997). However, anaerobic oxidation of methane by microbes effectively removes methane from marine sediments before it reaches the sediment-water interface (Hinrichs and Boetius, 2002, and references therein). The anaerobic oxidation of methane occurs simultaneously with organoclastic sulfate reduction. Figure 1 illustrates the stoichiometry of the overall microbially mediated transformation of carbon in the marine environment, showing the sulfate-methane transition zone (SMTZ). This zone acts as a barrier, preventing methane diffusion to the overlying water and then to the atmosphere. Moreover, the anaerobic oxidation of methane causes methane undersaturation in the sediment pore water and is thought to avert free gas formation near the sediment-water interface. This condition may even enhance methane dissolution into the water column above (Dale et al., 2008; Mogollón et al., 2009, 2011; Regnier et al., 2011). Thus, the anaerobic oxidation of methane plays a significant role in the regulation of the global methane budget and the emission of methane into the hydrosphere and atmosphere.

Assessing the causes and amount of methane production, oxidation, and transport in the Chukchi Sea requires a thorough evaluation of sediment geology, geochemistry, geophysics, and microbiology, including determination of methane turnover rates in sediments using geological and geochemical methods.

BACKGROUND

The first data sets on hydrocarbon gases in the uppermost sediment of the Chukchi Sea were obtained from 1976 to 1984 during repeated expeditions of NIIGA-VNIIOkeangeologia Russian research institution (Yashin et al., 1981, 1985). The study focused on the discovery of indicators of deep thermogenically formed gas. These indicators in the sediments were used to estimate the hydrocarbon potential in the Russian (western) sector of the Chukchi Sea. Preliminary results showed that relatively wide regions of the western Chukchi seafloor exhibit elevated levels

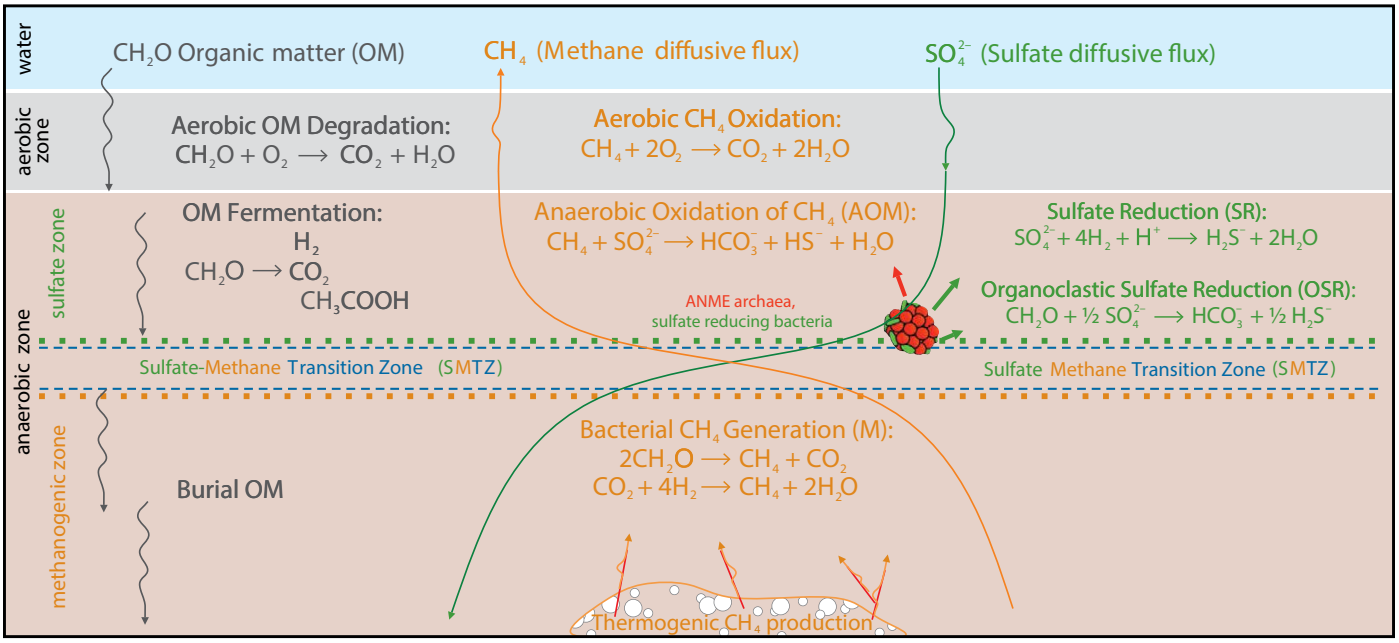

FIGURE 1. Sketch representing microbially mediated processes of organic matter transformation in marine sediments. (left) Organic matter (OM, represented as CH_2O) deposited on the seafloor is aerobically degraded to CO_2 and H_2O. In the sulfate zone, OM is anaerobically transformed by fermentation to hydrogen (H_2), carbon dioxide (CO_2), and smaller organic compounds (represented as acetate, CH_3COOH). (right) Hydrogen produced during OM fermentation fuels sulfate reduction (SR) in anoxic sediments. Organoclastic SR is the net reaction for sulfate reduction and OM fermentation. (center) Hydrogen produced during OM fermentation fuels methane (CH_4) generation (MG). Methane may be anaerobically and/or aerobically oxidized or emitted to the water column. Anaerobic oxidation of methane (AOM) is mediated by a consortia of microbes that use sulfate as electron acceptors. These consortia consist of sulfate-reducing bacteria (stained green) and anaerobic methanotrophic (ANME) archaea (stained red). AOM consortia reduce sulfate, oxidize methane, and generate sulfide and bicarbonate. AOM leads to inhibition of the reaction by increased dissolved inorganic carbon (DIC) and sulfide. The green and blue arrows represent sulfate and methane diffusive fluxes and show typical sigmoidal curves that define the sulfate-methane transition zone (SMTZ)—the horizon where methane and sulfate are depleted simultaneously. The depth of the SMTZ depends on the consumption rate of sulfate and the flux of methane from below.

of hydrocarbon gases (mainly methane) that could be correlated with high hydrocarbon productivity in the source rocks below. Methods used in these historical studies included determining the molecular composition of hydrocarbon gases and developing methane concentration profiles, and then correlating them with the organic matter content and lithological characteristics of the gas-containing sediments. Most elevated concentrations of gases in sediments were confined to the South Chukchi Basin and, particularly, to Hope Deep, where the highest sedimentary methane concentrations were found. Though this research revealed a few methane "hotspots" within the Chukchi Sea (Yashin and Kim, 2007), no investigations of methane turnover in the sediment and water column were conducted.

The Russian-American Long-term Census of the Arctic (RUSALCA) was the first multidisciplinary collaboration between US and Russian scientists in more than a decade in the Chukchi Sea. This bilaterally supported program collected the first data that allowed study of the relationships among key microbial processes, methane formation, and turnover in both the water column and the sediments of the Chukchi Sea (Lein et al., 2007; Savvichev et al., 2007). In particular, elevated methane concentrations measured in an extension of Herald Canyon (Savvichev et al., 2004) were thought to indicate possible methane seepages through faults. As a result, methane emission from the water column into the atmosphere was estimated to range from 5.4–57.3 μmol CH_4 m^{-2} day^{-1}. During the RUSALCA 2009 and 2012 missions, the methane investigation focused on the origin of the gas in sediments and seawater. These data, coupled with the historical data set from NIIGA-VNIIOkeangeologia, form the basis for the present study.

This paper synthesizes all of the available methane data collected from the Chukchi Sea sediment and water column and determines the role of methane turnover and net transport within organic-rich environments along the shallow Chukchi shelf. We present for the first time spatial variation in methane concentration in surficial sediments and the water column, as well as implications for the origin of the methane. In this paper, we: (1) evaluate the anaerobic oxidation of methane, sulfate reduction, and methane gas generation rates by sampling (a) the concentration of methane with depth in the sediment, and (b) the pore water sulfate and organic matter content at two distinct Chukchi Sea sites; (2) determine whether or not sulfate reduction, which correlates with degradation of organic matter at the sediment surface, affects the distribution of sulfate and methane in the sediment; (3) estimate methane flux from the sediment; and (4) provide a retrospective review of methane distribution in the surficial sediments of the Chukchi Sea with respect to its potential transfer to the hydrosphere and atmosphere.

GEOLOGICAL SETTING OF THE CHUKCHI SEA

Tectonic events in the Caledonian (490–390 million years ago) and Late Mesozoic (66 million years ago) affected the part of the Chukchi shelf we surveyed. The shelf zone of the South Chukchi Basin is underlain by Late Mesozoic folded basement, with sediment thicknesses of 4–7 km. In contrast, the north-south oriented North Chukchi Basin has sediment fill up to 20–22 km thick (Vinogradov et al., 2006; State Geological Map of Russian Federation, 2006). These two basins, which differ in age and size, are divided by the structural Wrangel-Herald Uplift (also know as the Herald Arc; Grantz et al., 1975; Thurston and Theiss, 1987; Miller et al., 2002).

Our study area was primarily the western Chukchi Sea, which is bounded to the north by the 100 m isobath. The principal geological/morphological structures of the area include the South Chukchi Basin (a northwestern extension of the Kotzebue and Hope Basins of the United States [eastern] sector of the sea) and the northern extension of Herald Canyon in the North Chukchi Basin, where a very large hydrocarbon potential is proposed (Figure 2) (Verzhbitsky et al., 2008; Malyshev et al., 2011). Herald Canyon is a narrow inward-facing fault-bounded valley with a maximum depth of about 100 m on the shelf. It is considered to be a part of the greater Hope Valley-Herald Canyon drainage system that developed during the Pleistocene glacial maxima when sea levels were far lower than today. The South Chukchi Basin includes the Longa, North Schmidt, South Schmidt, Kolyuchinskaya, and Hope en echelon deeps divided by linear swells (Onman, Inkigur, and others; Figure 2). The Onman and Inkigur swells are thought to create structural sediment traps for the adjacent Hope, South Schmidt, and Kolyuchinskaya structures that contain Cretaceous and Paleogene gas source rocks (Kim et al., 2007; Malyshev et al., 2011). Seismic evidence showing changes in phase or polarity of seismic horizons and listric fault planes in the pre-rift sequences are associated with areas of reduced reflectivity, suggesting the presence of gas in the upper sediments of the basin (Verzhbitsky et al., 2008). Fault geometry indicates an extensional/transtensional setting for the South Chukchi rift basin, similar to the Hope Basin in the US part of the Chukchi Sea (Tolson, 1987).

There is evidence of several marine regressions and transgressions related to either tectonic or glacio-eustatic processes in Bering Strait and on the Chukchi shelf (Brigham-Grette and Carter, 1992; Svitoch and Taldenkova, 1994). In the final phase of basin development during the Pliocene and Quaternary (5.3 million years ago), regional subsidence occurred in the South Chukchi Basin that was not accompanied by faulting (Malyshev et al., 2011). The upper Pliocene-Quaternary sediment sequence is not faulted extensively, and today there is relatively low seismicity in the region with the exception of the most southern part of the Chukchi Sea and Barrow Canyon to the north (Composite Earthquake Catalog,

http://quake.geo.berkeley.edu/cnss). This quiescence implies an absence of modern tectonic events that could create gas migration pathways (faults, weak zones) for the methane sink within the seafloor.

Glacio-eustatic processes, ice scouring, and the general pattern of currents entering from the Bering Sea (Anadyr Water, Alaskan Coastal Water, Central Bering Shelf Water) control sedimentation in the region (Weingartner et al., 2005). North of Bering Strait, the throughflow exerts important influences at both regional and global scales. Because the shelf is strongly influenced by the advection of nutrient-rich waters from the Pacific Ocean, it sustains some of the highest benthic faunal soft-bottom biomass in the world. As reported by Grebmeier et al. (2006), high primary production over the shallow shelf results in the deposition of high levels of organic material to the seafloor.

STUDY SITES AND METHODS

The data discussed in this paper were obtained during the RUSALCA expeditions in 2004 (partly borrowed from Savvichev et al., 2007), 2009, and 2012 aboard the Russian R/V *Professor Khromov*. In addition, we incorporate a historical data set on methane content in surficial sediments from the 200 sampling stations obtained by NIIGA-VNIIOkeangeologia during expeditions in 1976–1984. Two sites with distinctly different geological settings and depositional patterns were chosen for detailed study. The northern site is located within the northern extension of Herald Canyon at a water depth of about 100 m. The southern site is located where the Kolyuchinskaya and Hope Deeps join in the South Chukchi Basin at about 50 m depth. Figure 2 shows the sampling stations and also the main geological/morphological structures. Survey methods during RUSALCA expeditions included sediment and water sampling and high-resolution seismic and side-scan surveys at the northern site.

Near-bottom water and surface horizons were sampled with five-liter bottles mounted on the rosette system provided by the Woods Hole Oceanographic Institution. In order to avoid air bubbles, the water samples were decanted from the bottles into glass containers, allowing the water to overflow on deck. The glass containers were then sealed with gas-tight stoppers. Methane concentration in the water samples was determined by using a Chrom-5 gas chromatograph equipped with a flame ionization detector.

A Russian-owned 330 cm hydraulic corer (GSP-2) was used for sediment coring. Cores were split immediately after recovery into one-meter sections and transferred to the shipboard laboratory for subsampling and processing. Pore water was squeezed from sediments samples using a pressure-filtration system within half an hour of core retrieval and then conserved for analysis on land. All the water and sediment sampling and subsampling procedures were carried out within a few hours of collection at a temperature close to in situ, ranging from −1.0° to +6°C. Appendix A describes the geochemical analyses techniques used.

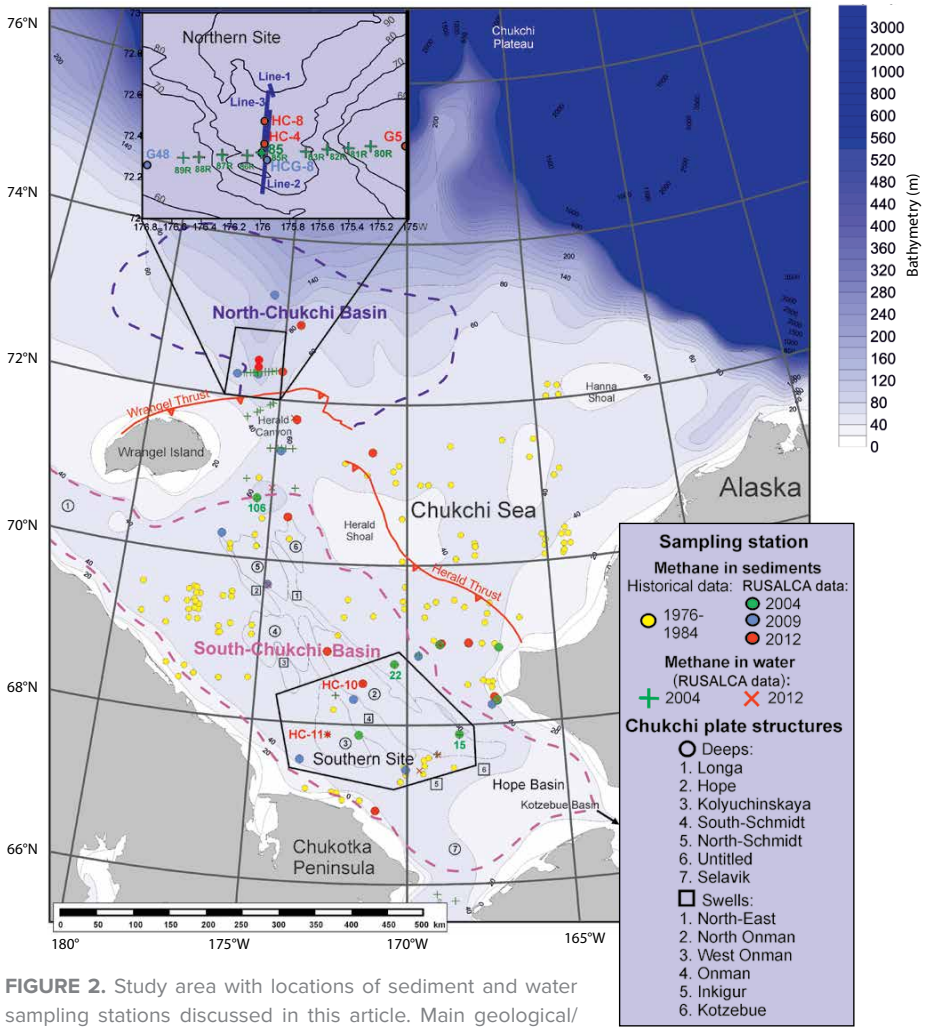

FIGURE 2. Study area with locations of sediment and water sampling stations discussed in this article. Main geological/morphological structures are indicated by circled and squared numbers, and North and South Chukchi Basin limits are indicated by dashed lines (compiled from Kim, 2004; State Geological Map of Russian Federation, 2006; Blackbourn Geoconsulting, 2015). Yellow dots are historical surficial sediment stations sampled by VNIIGA-VNIIOkeangeologia. Russian-American Long-term Census of the Arctic (RUSALCA) 2004, 2009, and 2012 coring stations are indicated by green, blue, and red dots, respectively. Green and red crosses are RUSALCA 2004 and 2009 water sampling stations. (Inset) Enlarged area of the northern site, with location of side-scan sonar and subbottom profiler survey lines (blue) and RUSALCA sampling stations. Isobaths are in meters (IBCAO). The RUSALCA station numbers are referenced throughout this paper.

High-resolution seismic data were acquired using a VNIIOkeangeologia SONIC-3M deep-towed system (side-scan sonar combined with 3.5 kHz subbottom profiler) along three track lines north from Herald Canyon (each over 100 km long) to characterize the upper sedimentary layers within the northern site.

RESULTS AND DISCUSSION

Methane in the Sediment

Methane in marine sediments can either be dissolved in pore waters or—in a case where in situ saturation is exceeded—exist as a free gas (Fleischer et al., 2001). The saturation level is controlled by pressure, temperature, and salinity (Yamamoto et al., 1976). The average methane concentration measured in sediment from the northern site (coring stations HC-4 and HC-8) is 0.0007 mM, three orders of magnitude less than methane solubility limit (3.7 mM at a pressure of 1.1 MPa). Water temperature was –1.85°C (Pickart et al., 2009) and pore water salinity was 30.4‰. The limit of methane solubility at station HC-10 in the southern site (Figure 2) was about 2.3 mM with pressure of 0.65 MPa, water temperature in the range of –1.8 ± 1.3°C (Lebedev et al., 2014), and pore water salinity of 29.0‰. Thus, the maximum methane concentration measured in core HC-10 (1.67 mM) is close to the saturation limit. However, no direct evidence of seep formation was detected at any of the study sites, suggesting upward methane transport mainly by diffusion and not by convection.

Statistical analysis of data from 200 coring stations obtained in the Chukchi Sea during the 1970s and 1980s shows average background methane concentrations (in the 0–4 m sediment section) of 0.0015 mM, with an outlier value of 0.0338 mM. The highest reported methane concentration is 0.1082 mM (Yashin et al., 1981, 1985). The data generally reflect a diffusely scattering methane background signal in the sediment and provide a reference value for comparison with the anomalously high values within our study area.

Figure 3A presents all of the available depth profiles of methane concentrations, Figure 3B plots pore water sulfate ion concentrations in the cores, and Figure 3D shows organic carbon content. The methane and sulfate concentration profiles demonstrate that the study sites are characterized by different sulfate reduction and methanogenesis processes. The South Chukchi Basin is the site of the highest methane concentration, reaching 2 mM at the HC-10 and HC-11 coring stations in the depth interval of 100–150 cm below the seafloor (cmbsf). Because sulfate is an electron acceptor, the anaerobic oxidation of methane is limited to the zone where sulfate penetrates and overlaps with methane. In diffusive systems, the activity of the anaerobic oxidation of methane can be depicted as a typical concave-up profile of methane concentration (observed in cores from stations HC-10 and HC-11). Three other stations (22, 15, and 106), located at the margins of the South Chukchi Basin, are characterized by moderate to low methane content and insignificant downcore increasing concentrations trends.

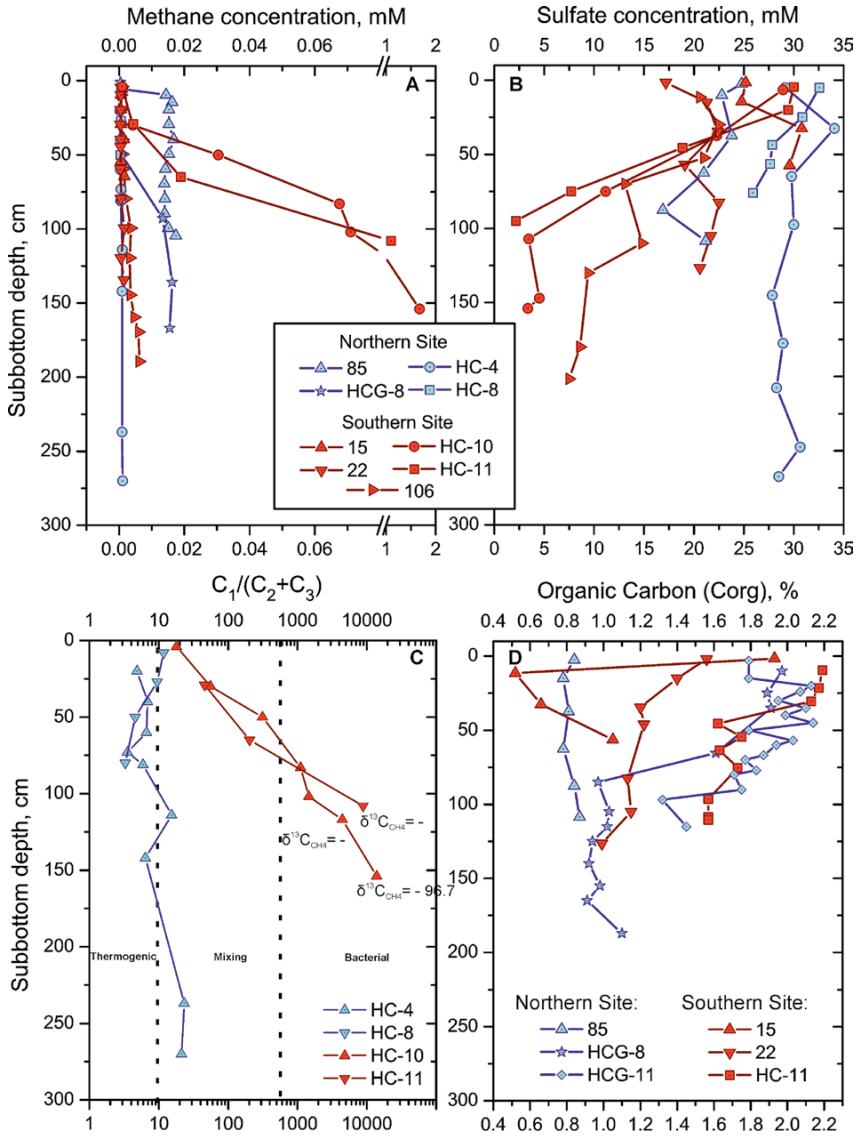

FIGURE 3. Depth profiles of (A) methane concentration in sediment, (B) pore water sulfate concentrations, (C) Bernard value ($C_1/(C_2+C_3)$), and (D) organic carbon content measured in the South Chukchi Basin (red symbols) and in the northern extension of Herald Canyon (blue symbols). Data from stations 15, 22, 85, and 106 are borrowed from Savvichev et al. (2007). Isotope compositions of methane carbon ($\delta^{13}C_{CH4}$) measured from HC-10 and HC-11 cores are indicated.

At the northern site, the highest methane concentrations were measured in the HCG-8 and -85 cores, with a maximum of about 0.02 mM at depths greater than 50 cm downcore. There is also a corresponding decrease in organic carbon at the same depth interval. This relatively low methane content at the northern site compared to the southern site is still higher than the background methane concentration in Chukchi Sea sediment.

Hydrocarbon Gases: Composition and Origin

Methane of both thermogenic and biogenic origin is characterized by a specific range of $\delta^{13}C$ values as well as by the proportion of co-occurring higher hydrocarbons (C_2, C_3…). Molecular analyses of sediment gases show distinct differences between the northern and southern sites. In cores HC-10 and HC-11 (southern site), methane is the dominant gas (98% and 99% of total hydrocarbons, respectively). The predominance of methane and C_1/C_2+C_3 (Bernard ratio) higher than 10,000 indicates a microbial origin for the gases studied (Bernard et al., 1978; Figure 3C). It should be noted that the diminishing $C_1/(C_2+C_3)$ ratios in the upper sediments can be explained as a result of (1) diagenesis, wherein amounts of C_2 and C_3 increase with depth, and/or (2) preferential loss of methane during outgassing. For example, during core recovery, methane saturates the pore fluid and is preferentially lost, while the other hydrocarbon gases, which are present in much lower concentrations, do not reach saturation and thus are retained in the pore waters. Partial methane outgassing affects methane concentrations and the $C_1/(C_2 + C_3)$ ratios but not methane carbon isotopic compositions. The isotopic compositions of $\delta^{13}C(CH_4)$ measured in cores HC-10 and HC-11 vary from –96.7‰ to –92.8‰, verifying a biogenic origin of the methane.

The northern site cores show quite a different picture. The amount of methane in the HC-8 and HC-4 cores is 83% and 85%, respectively. The heavy hydrocarbons are represented by ethylene (about 10%), i-butylene (1.7%), and a combination of ethane, propane, n-butane, and other hydrocarbons (1%). Unfortunately, isotopic measurements of methane ^{13}C were not performed at this site due to the limited volume of gas samples; however, a considerable amount of heavy hydrocarbon gases with a C_1/C_2+C_3 ratio less than 500 indicates mixed thermogenic-biogenic origin of the gases (see Figure 3C). The reduced C1/(C2+C3) value in the upper 50 cmbsf results from methane oxidation in the upper sediment layer (aerobic zone; see Figure 1; Hachikubo et al., 2015).

Specific Features of Gas-Containing Sediments

Northern Site

A geophysical survey at the northern site revealed a continuous enhanced reflector in the subseafloor (Figure 4). The depth of this reflector varies from 2 to 8 meters below the seafloor (mbsf), and its exact geologic nature is ambiguous. It may indicate the presence of gas or a sedimentological heterogeneity induced by changes in sediment deposition rate and changing in situ temperature regimes. We suggest that the reflector is relict seafloor permafrost that formed when sea level was much lower juxtaposed on a more modern layer of non-permafrost marine sediment. According to seismo-stratigraphic data reported in Gusev et al. (2009), a similar seismic reflector was identified south of Wrangel Island and offshore the Chukotka

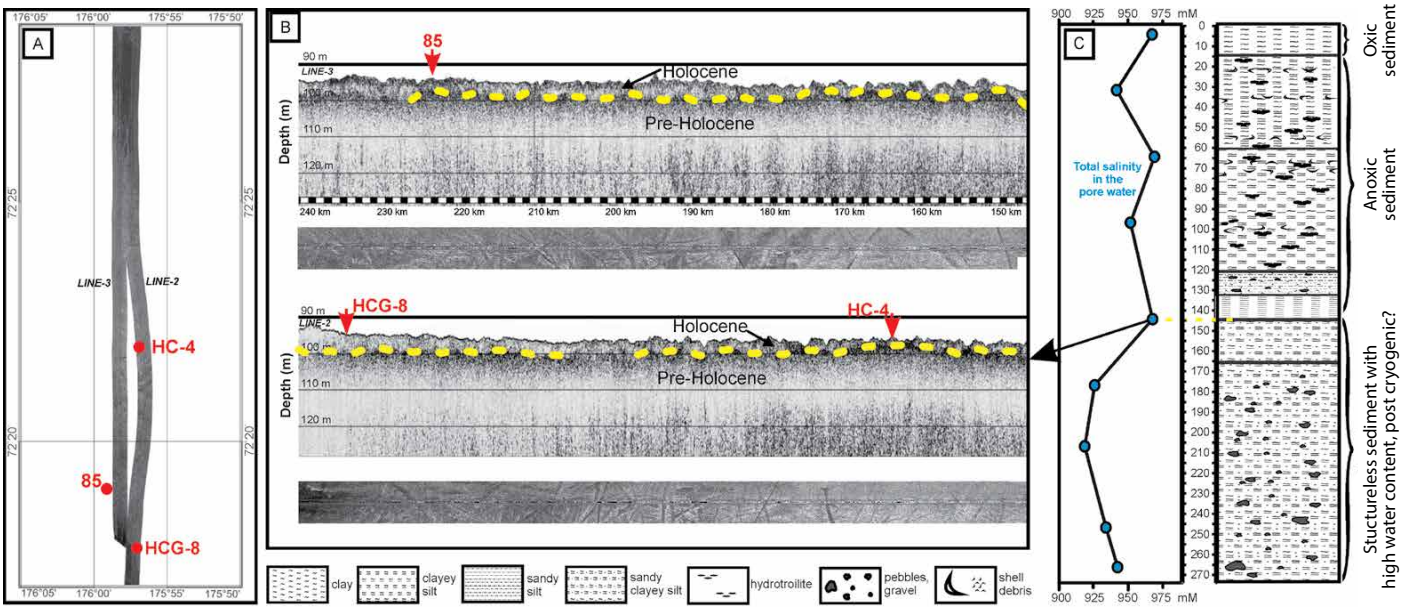

FIGURE 4. (A) Side-scan sonar lines acquired at the northern site. (B) Subbottom profiles and corresponding side-scan sonar lines in the vicinity of northern site coring stations 85, HC-4, and HCG-8; side-scan sonar swath is 1,500 m. Yellow dashed line is suggested pre-Holocene–Holocene boundary. (C) Lithological description (right) and depth pore water salinity distribution of core CH-4 (left).

Peninsula. This reflector is interpreted to be the Pleistocene-Holocene boundary on the basis of radiocarbon dating and borehole lithostratigraphy.

The SONIC-3M side-scan sonar images reveal a series of gouges, probably a consequence of iceberg keels plowing through the sedimentary seabed (see swaths in Figure 4B below the subbottom profiles). Such seafloor features have been identified in other areas of the Chukchi shelf where the seabed is as deep as 60 m, but they are most abundant at depths of 25–40 m (Phillips and Reiss, 1985; Phillips et al., 1988). In addition, Dove et al. (2014) reported that Chukchi shelf ice gouges can be found down to a depth of 350 m. Similar ice gouges have also been located on the Chukchi Plateau at depths in excess of 500 m. The ice gouges imaged by our side-scan sonar at water depths of 100 m were probably made at a time when sea level was eustatically lower than at present. The longest core (HC-4, 270 cm) retrieved at the northern site supports our interpretation (Figure 4C, right). The upper section of the core was deposited during the Holocene and includes an oxic-anoxic interface at 15 cmbsf and fine-grained anoxic sediments with hydrotroilite lenses and minor sand admixture (in its lower part) in the 15–135 cm depth interval. At an additional 15 cm downcore, a sandy silt layer reflects a change in the deposition regime during the last glacial regression. The lower section of the core is structureless, with very wet sandy silt and numerous pebbles, gravel, and debris, resembling a post-glacial environment such as an open coastal region or delta. During the sea level lowstand, the shelf was subaerially exposed, and ice-bonded permafrost may be have formed in the sediments. Reflooding of the frozen sediments with saline ocean waters likely triggered full or partial permafrost melting (Danilov et al., 1998). The pore water salinity distribution in this core (Figure 4C, left) shows that local freshening is confined to the lower core section, suggesting possible influence of freshwaters that could have saturated the sediments during shelf denudation at the time of regression.

Southern Site

There is no geophysical indication of gas-related features in the surficial sediment at the southern site, suggesting that the rate of methane turnover is proceeding in an anoxic environment laden with a high concentration of black iron sulfides. Reduced sulfur is not incorporated into the bacterial cells within the samples. In particular, cores HC-10 and HC-11 retrieved from the Hope and Kolyuchinskaya Deeps were characterized by a strong H_2S odor, numerous shells, and bioturbation, indicating very active sulfate reduction near the sediment-water interface.

Numerical Simulation of Methane Turnover

A numerical transport-reaction model, based on microbially mediated reactions, was used to simulate the degradation of organic matter in anoxic marine sediments studied in order to predict rates of anaerobic oxidation of methane, sulfate reduction, and methanogenesis (illustrated in Figure 1). Sediment cores HC-4 and HC-10 representing the characteristic features of the northern and southern sites, respectively, were chosen for the modeling efforts. Figures 2 and 3 show core locations and species distribution patterns. Appendix B provides a detailed description of the model. Tables 1 to 3 provide descriptions of the parameters and variables used for modeling. The organic matter content and transformation conditions as well as sedimentation rates are considered the most important parameters affecting the rates of microbially mediated methane turnover.

Organic Matter in Sediments

Organic carbon content is highly heterogeneous throughout the Chukchi Sea, and likely depends on the hydrodynamics of the water masses as they move through the narrow Bering Strait toward the Arctic Ocean. The average organic carbon value in the South Chukchi Basin is estimated to be 1.9%, with the largest organic carbon concentration (up to 2.57%) occurring south of South Schmidt

TABLE 1. Depth-dependent constitutive equations used in the modeling.

PARAMETER	CONSTITUTIVE EQUATION	NOTES
Porosity with depth	$\varphi(z) = \varphi_0 \cdot \exp(-\varphi_a \cdot z)$	φ_0 = porosity at the sediment surface φ_a = porosity-depth attenuation coefficient (Athy's law)
Molecular diffusion in sediments	$Ds = \theta\tau_L D_L$	τ = tortuosity is calculated by the Millington and Quirk (1961) model used in *Comsol Multiphysics* D_L = molecular diffusion coefficient is calculated by C.CANDY considering sediment pressure, temperature, and salinity (http://visumod.freeshell.org/thermo/difcoef.html)
Rate of fluid advection through the sediment	$u(z) = (v_f \cdot \varphi_f - u_0 \cdot \varphi_0)/\varphi(z)$	v_f = sedimentation rate φ_f = porosity at great sediment depth u_0 = upward rate of fluid flow at the seafloor (Luff and Wallmann, 2003)
Kinetic constant of organic matter degradation	$k_{OMD} = 0.16 \cdot (a_0 + z/v_f)^{0.95}$	a_0 = the initial age of organic matter degradation z = depth (Middelburg, 1989)
Factor converting G (wt%) into C (mol m^{-3})	$(1 - \varphi(z)) \cdot ds/(\varphi(z) \cdot Mc)$	ds = average density of dry solids Mc = molecular weight of OM ($CH_{h2}O$)

Deep. The average organic carbon content in the surficial sediments from the northern site is estimated to be 1.8%, with maximum values up to 2.38% in its southern and northern parts (Kolesnik and Mar'yash, 2011; Astakhov et al., 2013). Organic matter concentrations are related to sediment grain size and range from 0.05% in coarse-grained deposits to 2% in fine-grained sediments (Lysitsin, 1969; Walsh, 1989).

Almost all the cores collected at the southern site exhibit high levels of organic carbon, with the exception of station 15 (Figure 3D). The northern HC-4 core consists mainly of coarse-grained sediment and large-size ice-rafted debris, suggesting quite a low organic carbon value, similar to that measured at coring station 85 (0.85%; Figure 3D). Descriptions of organic matter parameters used during the modeling and the kinetics of organic matter degradation are given in Table 3 and Appendix C, respectively.

TABLE 2. Rate expressions and Rate laws applied in the differential equations.

SPECIES/RATE	RATES/KINETIC RATE LAW
Methane (CH_4)	$R_{(CH4)} = +R_{MG} - R_{AOM}$
Sulfate (SO_4)	$R_{(SO4)} = -R_{SR} - R_{AOM}$
DIC ($CO_3 + HCO_3 + CO_2$)	$R_{(DIC)} = R_{AOM} - (1 - f_{SO4}) \cdot R_{OMD} + R_{OMD}$
Organic matter degradation	$R_{OMD} = k_{OMD} \cdot C_{(CH2O)}$
Sulfate reduction	$R_{SR} = -R_{AOM} - f_{SO4}^{(1)} \cdot R_{OMD}$
Methanogenesis	$R_{MG} = -R_{AOM} + (1 - f_{SO4}) \cdot K_{in}^{(2)} \cdot R_{OMD}$
Anaerobic oxidation of methane	$R_{AOM} = k_{AOM} \cdot C_{(SO4)} \cdot C_{(CH4)}$

[1] f_{SO4} is a factor which controls the partitioning rate of OM degradation between organoclastic SR and MG, such that $f_{SO4} = C_{(SO4)}/K_{SO4}$ when $C_{(SO4)} < K_{SO4}$ and $f_{SO4} = 1$ when $C_{(SO4)} > K_{SO4}$, K_{SO4} is the half-saturation constant for sulphate (Mogollon et al., 2012).

[2] $K_{in} = K_c/(C_{(DIC)} + C_{(CH4)} + K_c)$, K_{in} is the factor that inhibits organic matter degradation in anoxic sediments, K_c is the Monod inhibition constant, $C_{(DIC)}$ is the concentration of dissolved inorganic carbon ($CO_3 + HCO_3 + CO_2$), and $C_{(CH4)}$ is the methane concentration (Wallman et al., 2006).

Sedimentation Rates

Study of sediment cores and seismic stratigraphy provide deposition patterns and sedimentation rates for the Chukchi Sea (Gusev et al., 2009, 2014). For the western part of this sea, Gusev et al. (2009) report relatively high early Holocene sedimentation rates of several meters per thousand years, which are common for the early stages of flooding on the Arctic shelf (e.g., Stein et al., 2004). Subsequently, deposition was greatly reduced to about one meter in ~9,000 years. Assuming the reflector observed in our seismic records is the pre-Holocene–Holocene boundary, Holocene sediment thickness varies from 2 to 8 m, suggesting sedimentation rates at the northern site in the range of 20–80 cm kyr^{-1}. In the vicinity of station HC-4, the pre-Holocene–Holocene boundary occurs at 2.5 m, suggesting sedimentation rates of 25 cm kyr^{-1} (see Table 3).

Overall sedimentation rates within the South Chukchi Basin during the Holocene were estimated as high as 200 cm kyr^{-1} (Viscosi-Shirley, 2000). This value was used for modeling the rate of methane turnover in the sediment at station HC-10 (see Table 3).

TABLE 3. Settings corresponding to the cores modeled in this study.

PARAMETER	SYMBOL [UNIT]	HC-4	HC-10
Bottom water temperature (temperature gradient 0.03°C/m)	T [°C]	–1.85	–1.8 – +1.3
Porosity at the sediment surface[1]	φ_0 [dimensionless]	0.6	0.7
Porosity-depth attenuation coefficient	φ_a [dimensionless]	0.001	0.001
Sedimentation rate	v_f [cm/a]	0.0025	0.2
Sediment density	ds [g/cm^3]	2.65	2.65
Rate of fluid advection through the sediment (at zero depth)	u(z) [cm/a]	0.03	0.19
Initial age of OM degradation	a_0 [a]	30000	0
The content of OM in surface sediments[2] (at zero depth)	OM [wt%]	1.7	4.4
Molecular mass of $C(H_2O)$	Mc [g/mol]	30	30
Inhibition constant of OM degradation	K_c [mM]	1	1
Kinetic constant of AOM	k_{AOM} [cm^3/(mmol·a)]	1	30
Molecular diffusion coefficient for methane[3] (at zero depth)	D_{CH4} [cm^2/a]	231	245
Molecular diffusion coefficient for sulfate[3] (at zero depth)	D_{SO4} [cm^2/a]	135	146
Methane solubility calculated by Henry's and Sechenov's laws (top/bottom)	Cms [mM]	3.7/14.3	2.3/14.4

[1] Below 146 cmbsf adopted 0.8 porosity due to watery sediments (for core HC-4)

[2] Organic matter content in sediment was defined by multiplying C_{org} value by constant 2 (GOST 23740-79 Soils)

[3] Diffusion coefficients for sulfate and methane in the sediment interval 0–25 cmbsf were identified as Heaviside functions with modeling domain upper boundary values: z = 0 cmbsf - 8D, z = 25 cmbsf – 1D, taking into account the settling of sulfate from seawater (Jørgensen and Parkes, 2010).

Contemporary Geochemical Concentrations and Turnover Rates

Here, we compare simulated methane and sulfate concentrations at the sampling stations to corresponding measured data, where available (Figure 5A,B). Figure 5C,D plots the rates of total sulfate reduction, methanogenesis, and anaerobic oxidation of methane.

Southern Site

Site HC-10 is characterized by intense diagenesis of organic material dominated by sulfate reduction. According to the simulation results, the upper 10 cm of the sediment column has the highest sulfate reduction rate. These results are in good agreement with visual observations (absence of an oxidizing layer, dark sediment color, and strong H_2S odor). It should be noted that within the upper 50 cm horizon, sulfate reduction occurs due to organic material degradation (sulfate reduction rates vary from 153 μmol dm^{-3} day^{-1} at the surface to 0.4 μmol dm^{-3} day^{-1} at 50 cmbsf). The good fit between measured and modeled sulfate reduction at 25 cmbsf supports the simulation data. From 50–225 cmbsf, sulfate reduction is due to both anaerobic oxidation of methane and degradation of organic material. The maximum rate of anaerobic oxidation of methane is 0.23 μmol dm^{-3} day^{-1}, and it occurs at the depth of 115 cmbsf.

It should be noted that in the depth interval of 110–150 cm, the modeled sulfate reduction rates are underestimated when compared to the measured data (Figure 5C). Indeed, the original downward sulfate flux from the seawater may be different from the value used by our simulation model due to sediment heterogeneity and/or strong bioturbation. On the other hand, the occurrence of microniches with depleted organic matter is quite possible. The niches may serve as potential local sulfate repositories within organic-rich reduced sediments.

Thus, the simulation shows that with increasing sediment depth, sulfate is completely consumed in the SMTZ until ambient saturation concentrations are reached. Methane generation begins at 190 cmbsf, with a maximum production rate of 0.06 μmol dm^{-3} day^{-1} at a depth of 215 cmbsf. The rate of methane generation at this depth is much higher than that measured at stations 15 and 22, which are located within the same basin structure (0.0075 and 0.012 μmol dm^{-3} day^{-1}, respectively; Savvichev et al., 2007). Methane's high anaerobic oxidation rate is a result of both highly diffusive and convective methane flux (about 0.2 cm yr^{-1}).

The observed sulfate reduction appears to be the primary process that prevents significant upward flux of methane from southern site sediments to the overlying water column. The simulation allows us to estimate the diffusive methane flux at the sediment-water interface within the southern site to be 14.5 μmol dm^{-2} day^{-1}.

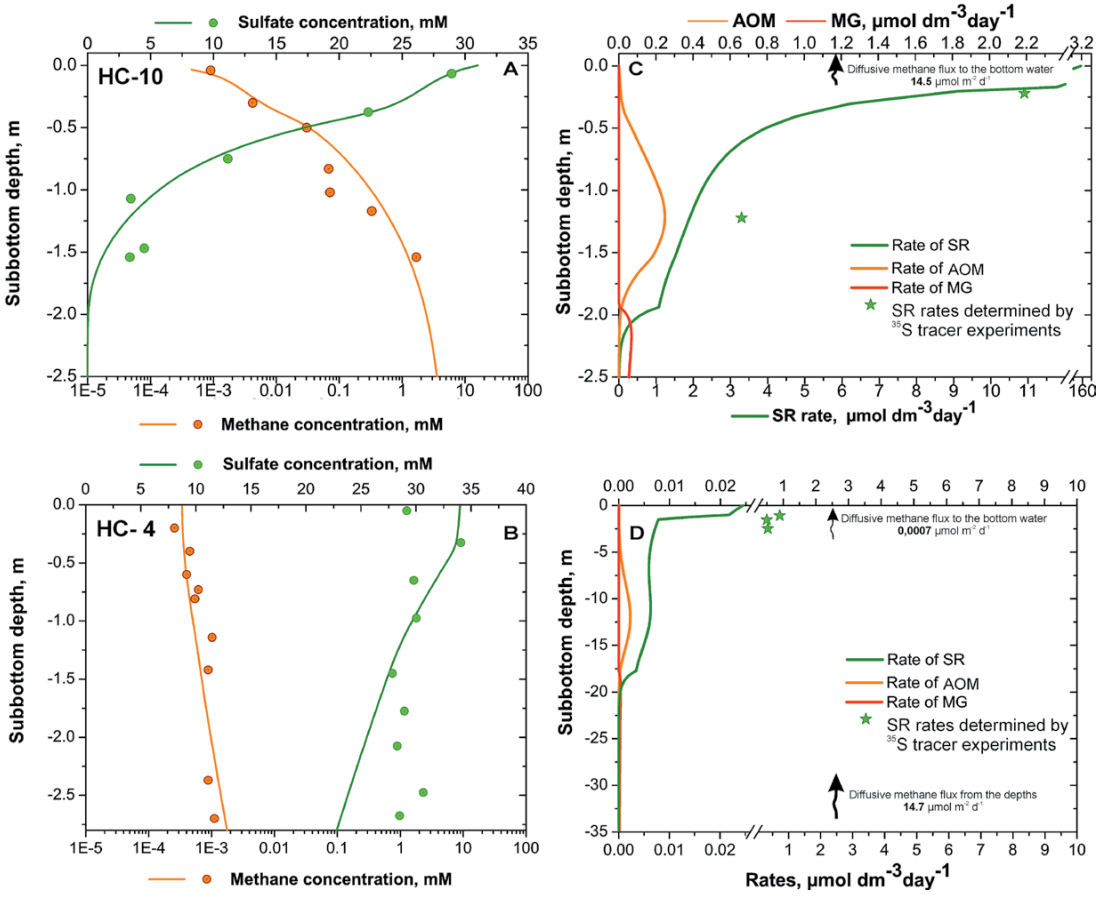

FIGURE 5. (A, B) Simulated methane (orange) and sulfate (green) profiles. Note that modeled methane concentrations were reduced by 50% in order to fit measured data by accounting for methane loss during core sampling and headspace subsampling. (C, D) Rates of sulfate reduction (green), AOM (orange), and methanogenesis (red) are plotted against the available measured data (orange dots = methane, green dots = sulfate) for stations HC-10 and HC-4. Estimated diffusive fluxes of methane are indicated.

Northern Site

As a whole, core HC-4 is characterized by low rates of diagenetic processes. According to the modeling and measurements in the upper Holocene sequence, the only sulfate reduction is occurring at a maximum rate of 0.02 μmol m^{-2} day^{-1}. Despite the fact that measured sulfate reduction rates are higher by about two orders of magnitude than the modeled rate, both measured and modeled sulfate reduction rates are low. At the same time, there is a good fit between measured and modeled sulfate reduction rates within the 150–250 cmbsf interval, reflecting a shift in the sulfate reduction rates. This shift is well described by changes of sediment lithology at the pre-Holocene–Holocene boundary (Figure 4C).

The model predicts a maximum methane anaerobic oxidation rate of 0.0026 μmol dm^{-3} day^{-1}) at a depth of 12 mbsf, corresponding to the late Pleistocene, and comparable to rates measured by Savvichev et al. (2007). However, the modeled CH_4 concentration at the predicted rate of anaerobic oxidation of methane appears to be underestimated. Assuming the origin of CH_4 at the northern site is due to vertical migration (Figure 3C), we used an upward diffusive methane flux of 14.7 μmol m^{-2} day^{-1} at the base of the modeled domain to reconcile the model with the measured amount of methane flux. Thus, according to the simulation, the northern site is characterized by a lengthy zone of anaerobic oxidation of methane occurring in the 7.5–17.7 mbsf interval. Bacterial methane production occurs immediately below the anaerobic oxidation of methane zone, reaching its maximum value of 0.0002 μmol dm^{-3} day^{-1} at 18.5 mbsf. Thus, the contribution of microbially mediated organic matter transformation into methane at the northern site is negligible. The main source of methane supplied to the water column is from deeply buried gas source rocks. The estimated diffusive methane flux at the sediment-water interface is as low as 0.7 nmol dm^{-2} day^{-1}.

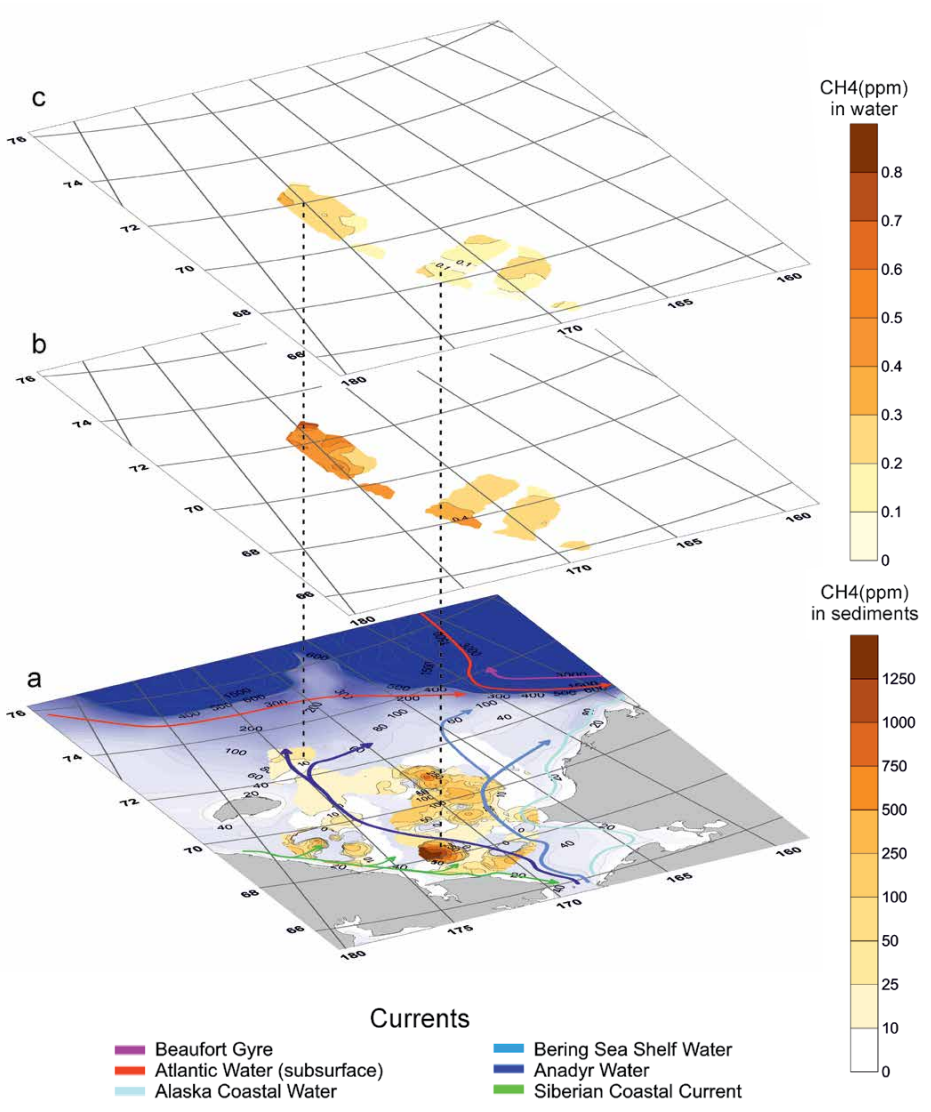

FIGURE 6. Spatial distribution of methane concentrations (a) in surficial sediments, (b) near bottom, and (c) in surface water horizons. The data were compiled from different sources (VNIIGA-VNIIOkeangeologia historical data; RUSALCA 2004, 2009, and 2012 data), and processed by a Kriging gridding method (regional bathymetry: IBCAO, Lambert projection). Current flow direction is from the online schematic Edge of the Arctic Shelf (2002).

Spatial Distribution of Methane in Sediment and Water and its Potential Transfer to the Hydrosphere

All the available data on methane distribution in the surficial sediments and those of the near-bottom and surface water horizons were mapped over the study area by using the Kriging geostatistical gridding method. It should be noted that historical data on methane content in the surficial sediments within the southwestern Chukchi shelf are in good to moderate correlation with RUSALCA measurements. Some discrepancy is obviously due to irregular distribution of sampling stations. Available data on methane concentration in surficial sediments (0–5 cmbsf) on the Chukchi shelf reveals methane "hotspots" occurring in the Kolyuchinskaya Deep (concentration of 1,250 ppm) in the South Chukchi Basin, and in a wide area in the central Chukchi Sea where methane concentrations reach 250 ppm. The northern site appears to be characterized by relatively low methane content in sediment (although it is higher than background values; see section on Methane in Sediment; Figure 6a).

Measurements of methane in the water column obtained during the RUSALCA 2004 and 2012 expeditions show that throughout the study area, methane concentrations in water just above the seafloor are higher than open-ocean background values in the Arctic (<0.096 ppm) (Damm et al., 2007); they vary from 0.1 ppm in the western part of the Chukchi Basin to 0.8 ppm in the northern extension of Herald Canyon. Analysis of the spatial distribution of methane concentrations in the near-bottom water layer show a systematic increase in Anadyr Water, extending from Bering Strait to the mouth of Herald Canyon. The same tendency occurs in the subsurface layer, with decreasing methane concentrations due to diffusion and oxidation (Figure 6a,b).

A juxtaposition of methane distribution maps (Figure 6a–c) shows that the spatial distribution of methane in surficial sediment does not correspond with that of water. It appears that methane concentrations measured in the water in Herald Canyon are higher than that of the South Chukchi Basin. Note that the season the observations were taken was not considered. Table 4 summarizes the minimum, average, and maximum CH_4 concentrations at both study sites (subsurface, near-bottom water, and surface water). These data show that dissolved methane is available for upward diffusion and oxidation. The calculations show that the higher the CH_4 content is in the subsurface sediments, the less it diffuses into the water column. This is related to high methane consumption via anaerobic oxidation of methane and sulfate reduction in the organic-rich sediments. However, at locations with low methane content in the surficial sediments, up to 60% of the methane budget enters the hydrosphere, indicating low methane consumption in the sediment. This is true only for the southern site—it is not observed at the northern site. It is remarkable that the thickness of the water column, which defines the overall range of CH_4 oxidation, has no significant influence on methane flux. In particular, despite the 50 m difference in water depth between the two study sites, the maximum surface water methane concentrations measured within Herald Canyon are still higher than they are at the southern site in the South Chukchi Basin. The data obtained allow us to estimate possible methane fluxes from the water to the atmosphere at the two sites using a diffusive methane flux in water of 0.13 nmol m^{-2} day^{-1} (Iversen and Jørgensen, 1985). Figure 7 summarizes the results of these balance calculations, which show almost equal CH_4 concentrations (0.3 and 0.4 ppm) and, consequently, equal methane flux from the water to the atmosphere at both sites, despite the differences in their environments.

The data suggest an additional source for methane water enrichment in Herald Canyon other than surficial sediment. Yet, methane oxidation rates in the water column estimated at Herald Canyon are higher than those in the South Chukchi Basin. We suggest that the enhanced methane content within Herald Canyon results from advection of methane-enhanced waters from the southern site via the Anadyr Current (Figure 6). Because hydrocarbon gas occurs dissolved in seawater, it can be transported laterally and vertically, in some cases over long distances (Johnson et al., 1993). Data on methane oxidation rates and methane concentrations in the water column at stations 22, 106, and 85 located along the Anadyr Current supports our hypothesis (Table 5). Taking into account the approximate time required for methane transport from the southern station 22 hotspot in the South Chukchi Basin to northern station 85 in the mouth of Herald Canyon using the velocity of the northward-flowing Anadyr Water, we calculated methane loss over the flow transfer. Data on Anadyr Water flow were taken from Baum (2011) and Pickart et al. (2009). Results show that the total volume of methane that could be oxidized during passage from station 22 to station 106 (distance of about 350 km, Anadyr Current speed of 30 cm s^{-1}, and transfer time of 14 days) and from station 106 to station 85 (distance of about 250 km, Anadyr Current speed of 50 cm s^{-1}, and transfer time of 6 days) is much less than the input concentrations, supporting our hypothesis (Table 5).

CONCLUSIONS

Shallow methane and the processes related to methane turnover were studied at two distinct sites in the Chukchi Sea. On the large scale, the differences between these sites are defined by different geological settings and sediment deposition regimes during the Pleistocene to Holocene.

TABLE 4. Spatial distribution of methane concentrations within the study sites.

CONCENTRATION, PPM/HORIZON	MINIMUM		AVERAGE		MAXIMUM	
STUDY SITE	NORTHERN	SOUTHERN	NORTHERN	SOUTHERN	NORTHERN	SOUTHERN
Surface water	0.18 (4.89%)	0.04 (16.00%)	0.41 (2.95%)	0.29 (0.27%)	0.41 (1.18%)	0.29 (0.02%)
Near bottom water	0.26 (7.07%)	0.15 (60.00%)	0.47 (3.38%)	0.31 (0.29%)	1.00 (2.88%)	0.80 (0.06%)
Surficial sediment	3.68 (100%)	0.25 (100%)	13.90 (100%)	107.48 (100%)	34.77 (100%)	1250.00 (100%)

(%) = remanded share of dissolved methane after loss during an upward diffusion and oxidation (assuming 100% methane concentration in the surficial sediment at the beginning of emission to the water column).

The northern site was subaerially exposed, possibly affecting the character of methane emission. Pre-Holocene sediments may have trapped diffusive thermogenic gas during the sea level lowstand. During basin subsidence and ocean transgression, the relict seafloor permafrost thawed, allowing methane to migrate. This gas originates from deeper sedimentary strata and mingles with additional microbial methane from the Pleistocene sediment sequence. However, rates of measured microbial methane generation do not match the predicted generation at the southern site. The diffusive methane flux at the sediment-water interface here is estimated to be as low as 0.7 nmol dm^{-2} day^{-1}. Thus, it should not be expected that this environment is a strong source of atmospheric CH_4. However, this study reveals some interesting insights into mechanisms of CH_4 fluxes at the northern site, which appear to be controlled by northward transport of CH_4 via ocean currents entering the Chukchi Sea through Bering Strait.

Evaluation of the rates of anaerobic oxidation of methane, sulfate reduction, and methane generation using measured and modeled data for the methane cycle transport-reaction provide insight into Holocene methane dynamics within the South Chukchi Basin. The southern site appears to be a consistent source of biogenic methane in the surficial sediments and the water column. The estimated diffusive methane flux at the sediment-water interface within the southern site is as high as 14.5 µmol dm^{-2} day^{-1}. Despite the fact that as much as 60% of the net flux was calculated to be lost through sediment-water gas exchange due to intensive microbial methane consumption, the South Chukchi Basin may serve as a supplementary source of methane emitted into the atmosphere at Herald Canyon.

It is clear that organic methane reaches surficial sediments in the Southern Chukchi Basin and is one of the important sources of atmospheric methane. Further work is required to accurately quantify this flux. New findings of methane seepage (convection) would lead to considerable upscaling of the methane shelf source compared to that based on diffusive fluxes alone.

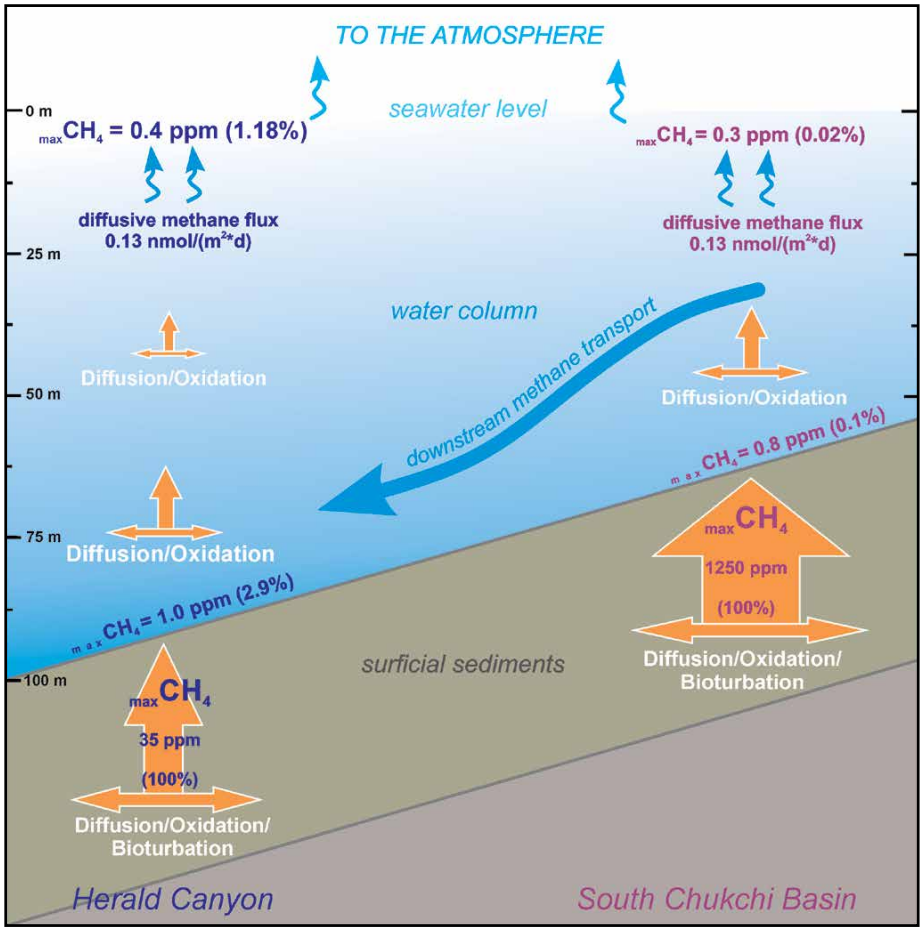

FIGURE 7. Illustration comparing methane flux dynamics at the northern Herald Canyon (values in blue) and southern sampling sites (values in pink). Max CH_4 reflects maximum of measured methane concentration, and % values represent methane transfer percentage in the corresponding horizon. Diffusive methane flux is calculated as the gradient of methane concentration from the bottom to surface waters, multiplied by the methane molecular diffusion coefficient of $8.7 \cdot 10^{9} m^2$ s^{-1} (Iversen and Jørgensen, 1993).

TABLE 5. Methane oxidation (MO) in the water column over flow transfer.

Station	Total MO (per m^2) Integrated Over Water Depth[1] (µmol m^{-2} day^{-1})	Water Depth (m)	Average MO Rates in Water Column (µmol m^{-3} day^{-1})	Average (max, min) Methane Concentration in Water Column (µmol m^{-3})	Methane Loss Over Flow Transfer (µmol m^{-3})	Methane Loss Over Flow Transfer (% from min concentration)
22	2.4	57	0.042	9.7 (7.1, 12.9)	1.2	13.4
106	9.8	72	0.136	16.2 (10.8, 20.0)		
85	17.7	103	0.172	15.7 (12.9, 17.1)	0.9	7.6

[1] Data from Savvichev et al. (2007)

REFERENCES

Astakhov, A.S., E.A. Gusev, A.N. Kolesnik, and R.B. Shakirov. 2013. Conditions of the accumulation of organic matter and metals in the bottom sediments of the Chukchi Sea. *Russian Geology and Geophysics* 54:1,056–1,070, http://dx.doi.org/10.1016/j.rgg.2013.07.019.

Baum, S. 2011. *Anadyr Current*, http://www.eoearth.org/view/article/150051 (accessed March 4, 2015).

Bernard, B.B., J.M. Brooks, and W.M. Sackett. 1978. Light hydrocarbons in recent Texas continental shelf and slope sediments. *Journal of Geophysical Research* 83(C8):4,053–4,061, http://dx.doi.org/10.1029/JC083iC08p04053.

Blackbourn Geoconsulting. 2015. *Enclosure 1. Chukchi Sea: Regional Structure and Location Map,* http://www.blackbourn.co.uk/reports/chukchi-sea.html.

Brigham-Grette, J., and J. Carter. 1992. Pliocene marine transgressions of northern Alaska: Circumarctic correlations and paleoclimatic interpretations. *Arctic* 45(1):74–89, http://dx.doi.org/10.14430/arctic1375.

Claypool, G.E., and I.R. Kaplan. 1974. The origin and distribution of methane in marine sediments. Pp. 97–139 in *Natural Gases in Marine Sediments*. I.R. Kaplan, ed., Plenum, NY.

Dale, A.W., P. Regnier, P. Van Cappellen, and D.R. Aguilera. 2008. Methane efflux from marine sediments in passive and active margins: Estimations from bioenergetic reaction–transport simulations. *Earth and Planetary Science Letters* 265:329–344, http://dx.doi.org/10.1016/j.epsl.2007.09.026.

Damm, E., U. Schauer, B. Rudels, and C. Haas. 2007. Excess of bottom-released methane in an Arctic shelf sea polynya in winter. *Continental Shelf Research* 27(12):1,692–1,701, http://dx.doi.org/10.1016/j.csr.2007.02.003.

Danilov, I.D., I.A. Komarov, and A.Yu. Vlasenko. 1998. Pleistocene-Holocene permafrost of the East Siberian Eurasian Arctic shelf. Pp. 207–212 in *PERMAFROST: Seventh International Conference (Proceedings).* Yellowknife, Canada, Collection Nordicana, No. 55.

Davis, A.M. 1992. Shallow gas: An overview. *Continental Shelf Research* 12(10):1,077–1,079, http://dx.doi.org/10.1016/0278-4343(92)90069-V.

Dove, D., L. Polyak, and B. Coakley. 2014. Widespread, multi-source glacial erosion on the Chukchi margin, Arctic Ocean. *Quaternary Science Reviews* 92:112–122, http://dx.doi.org/10.1016/j.quascirev.2013.07.016.

Edge of the Arctic Shelf. 2002. A schematic of the circulation over the Chukchi Sea and Beaufort/Chukchi slope, http://www.whoi.edu/arcticedge/arctic_west02/expedition/objectives.html.

Fleischer, P., T.H. Orsi, M.D. Richardson, and A.L. Anderson. 2001. Distribution of free gas in marine sediments: A global overview. *Geo-Marine Letters* 21:103–122, http://dx.doi.org/10.1007/s003670100072.

Gal'chenko, V.F. 1994. Sulfate reduction, methanogenesis, and methane oxidation in various water bodies of the Banger Hills Oasis, Antarctica. *Mikrobiologiya* 63(4):683–698). [in Russian]

GOST 23740-79. 1987. Soils: Methods of laboratory determination of organic composition. *Publisher Standards, Moscow*. [in Russian]

Grantz, A., M.L. Holmes, and B.A. Kososki, 1975. *Geologic Framework of the Alaskan Continental Terrace in the Chukchi and Beaufort Seas*. Open-File Report 75-124, US Geological Survey, 43 pp.

Grebmeier, J.M., L.W. Cooper, H.M. Feder, and B.I. Sirenko. 2006. Ecosystem dynamics of the Pacific-influenced Northern Bering and Chukchi Seas in the Amerasian Arctic. *Progress in Oceanography* 71:331–361, http://dx.doi.org/10.1016/j.pocean.2006.10.001.

Gusev, E.A., I.A. Andreeva, N.Y. Anikina, S.A. Bondarenko, L.G. Derevyanko, A.G. Iosifidi, T.S. Klyuvitkina, I.V. Litvinenko, V.I. Petrova, E.I. Polyakova, and others. 2009. Stratigraphy of Late Cenozoic sediments of the western Chukchi Sea: New results from shallow drilling and seismic-reflection profiling. *Global and Planetary Change* 68:115–131, http://dx.doi.org/10.1016/j.gloplacha.2009.03.025.

Gusev, E.A., N.Yu. Anikina, L.G. Derevyanko, T.S. Klyuvitkina, L.V. Polyak, E.I. Polyakova, P.V. Rekant, and A.Yu. Stepanova. 2014. Holocene paleoenvironment developments of southern part of Chukchi Sea. *Oceanology* 54(4):505–517.

Hachikubo, A., K. Yanagawa, H. Tomaru, H. Lu, and R. Matsumoto. 2015. Molecular and isotopic composition of volatiles in gas hydrates and in sediment from the Joetsu Basin, eastern margin of the Japan Sea. *Energies* 8:4,647–4,666, http://dx.doi.org/10.3390/en8064647.

Hinrichs, K.-U., and A. Boetius. 2002. The anaerobic oxidation of methane: New insights in microbial ecology and biogeochemistry. Pp. 457–477 in *Ocean Margin Systems*. G. Wefer, D. Billett, D. Hebbeln, B.B. Jørgensen, M. Schlüter, and T. Van Weering, eds, Springer-Verlag Berlin Heidelberg.

Isaksen, I.S.A., M. Gauss, G. Myhre, K.M.W. Anthony, and C. Ruppel. 2011. Strong atmospheric chemistry feedback to climate warming from Arctic methane emissions. *Global Biogeochemical Cycles* 25:1–11, http://dx.doi.org/10.1029/2010GB003845.

Iversen, N., and B.B. Jørgensen. 1985. Anaerobic methane oxidation rates at the sulfate-methane transition in marine sediments from Kattegat and Skagerrak (Denmark). *Limnology and Oceanography* 30(5):944–955, http://dx.doi.org/10.4319/lo.1985.30.5.0944.

Iversen, N., and B.B. Jørgensen. 1993. Diffusion coefficient of sulfate and methane in marine sediments: Influence of porosity. *Geochimica et Cosmochimica Acta* 57:571–578, http://dx.doi.org/10.1016/0016-7037(93)90368-7.

Johnson, V.G., D.L. Graham, and S.P. Reidel. 1993. Methane in Columbia River Basalt aquifers: Isotopic and geohydrologic evidence for a deep coal-bed gas source in the Columbia Basin, Washington. *AAPG Bulletin* 77:1,192–1,207.

Jørgensen, B.B., and R.J. Parkes. 2010. Role of sulfate reduction and methane for anaerobic carbon cycling in eutrophic fjord sediments (Limfjorden, Denmark). *Limnology and Oceanography* 55:1,338–1,352, http://dx.doi.org/10.4319/lo.2010.55.3.1338.

Judd, A.G. 2003. The global importance and context of methane escape from the seabed. *Geo-Marine Letters* 23:147–154, http://dx.doi.org/10.1007/s00367-003-0136-z.

Judd, A.G., and M. Hovland. 2007. *Submarine Fluid Flow: The Impact on Geology, Biology, and the Marine Environment*. Cambridge University Press, 475 pp.

Kim, B.I. 2004. Chukchi Sea: Sedimentary cover thickness and main structural elements. Pp. 1–7 in *Geology and Mineral Resources of the Russian Shelf Areas* (atlas). Scientific World, Moscow.

Kim, B.I., N.K. Evdokimova, O.I. Suprunenko, and D.S. Yashin. 2007. Oil geologic zoning of offshore areas of the east Arctic seas of Russia and their oil and gas potential prospects. *Oil and Gas Geology* 2:49–59. [in Russian]

Kolesnik, A.N., and A.A. Mar'yash. 2011. Organic carbon in the surface layers of bottom sediments in the Chukchi and adjacent seas. *Investigated in Russia* 14:15–20, http://www.sci-journal.ru/articles/2011/003.pdf. [in Russian]

Lebedev, N.V., S.V. Karpij, and V.Y. Karpij. 2014. Atlas of the Chukchi Sea thermohaline characteristics: 2014, http://www.aari.ru/resources/a0013_17/chukchi/atlas_start.htm [in Russian]

Lein, A.Yu., A.S. Savvichev, I.I. Rusanov, G.A. Pavlova, N.A. Belyaev, K. Craine, N.V. Pimenov, and M.V. Ivanov. 2007. Biogeochemical processes in the Chukchi Sea. *Lithology and Mineral Resources* 42(3):221–239, http://dx.doi.org/10.1134/S0024490207030029.

Luff, R., and K. Wallmann. 2003. Fluid flow, methane fluxes, carbonate precipitation and biogeochemical turnover in gas hydrate-bearing sediments at Hydrate Ridge, Cascadia Margin: Numerical modeling and mass balances. *Geochimica et Cosmochimica Acta* 67:3,403–3,421, http://dx.doi.org/10.1016/S0016-7037(03)00127-3.

Lysitsin, A.P. 1969. *Recent Sedimentation in the Bering Sea*. Academy of Sciences of the USSR, 614 pp. [in Russian]

Malyshev, N.A., V.V. Obmetko, A.A. Borodulin, E.M. Barinova, and B.I. Ikhsanov. 2011. Tectonics of the sedimentary basins in the Russian sector of the Chukchi Sea. Pp. 203–2009 in *Proceedings of the International Conference on Arctic Margins VI (ICAM VI), Fairbanks, Alaska, May 2011*. University of Alaska Fairbanks.

Middelburg, J. 1989. A simple rate model for organic matter decomposition in marine sediments. *Geochimica et Cosmochimica Acta* 53:1,577-1,581, http://dx.doi.org/10.1016/0016-7037(89)90239-1.

Miller, E.L., M. Gelman, L. Parfenov, and J. Hourigan. 2002. Tectonic setting of Mesozoic magmatism: A comparison between northeastern Russia and the North American Cordillera. *GSA Special Paper* 360:313–332, http://dx.doi.org/10.1130/0-8137-2360-4.313.

Millington, R.J., and J.M. Quirk. 1961. Permeability of porous solids. *Transactions of the Faraday Society* 57:1,200–1,207, http://dx.doi.org/10.1039/TF9615701200.

Mogollón, J.M., A.W. Dale, H. Fossing, and P. Regnier. 2012. Timescales for the development of methanogenesis and free gas layers in recently-deposited sediments of Arkona Basin (Baltic Sea). *Biogeosciences* 9:1,915–1,933, http://dx.doi.org/10.5194/bg-9-1915-2012.

Mogollón, J.M., A.W. Dale, I. L'Heureux, and P. Regnier. 2011. Impact of seasonal temperature and pressure changes on methane gas production, dissolution, and transport in unfractured sediments. *Journal of the Geophysical Research* 116, G03031, http://dx.doi.org/10.1029/2010JG001592.

Mogollón, J.M., I. L'Heureux, A.W. Dale, and P. Regnier. 2009. Methane gas-phase dynamics in marine sediments: A model study. *American Journal of Science* 309:189–220, http://dx.doi.org/10.2475/03.2009.01.

Phillips, R.L., and T.E. Reiss. 1985. *Nearshore Marine Geologic Investigations, Point Barrow to Skull Cliff, Northeast Chukchi Sea*. Open-file Report 85-50, US Geological Survey, 22 pp.

Phillips, R.L., P. Barnes, R.E. Hunter, T.E. Reiss, and D.M. Rearik. 1988. *Geological Investigations in the Chukchi Sea, 1984, NOAA Ship* Surveyor *Cruise*. Open-file Report 88-25, US Geological Survey, 82 pp.

Pickart, R.S., L.J. Pratt, D.J. Torres, T.E. Whitledge, A.Y. Proshutinsky, K. Aagaard, T.A. Agnew, G.W.K. Moore, and H.J. Dail. 2009. Evolution and dynamics of the flow through Herald Canyon in

the western Chukchi Sea. *Deep-Sea Research Part II* 57:1–22, http://dx.doi.org/10.1016/j.dsr2.2009.08.002.

Portnov, A., A.J. Smith, J. Mienert, G. Cherkashov, P. Rekant, P. Semenov, P. Serov, and B. Vanshtein. 2013. Offshore permafrost decay and massive seabed methane escape in water depths >20 m at the South Kara Sea shelf. *Geophysical Research Letters* 40:1–6, http://dx.doi.org/10.1002/grl.50735.

Reeburgh, W.S. 1996. "Soft spots" in the global methane budget. Pp. 334–342 in *Proceedings of the 8th International Symposium on Microbial Growth on C-1 Compounds*, San Diego, CA, USA, 27 August–1 September, 1995. M.E. Lidstrom and F.R. Tabita, eds, Kluwer Academic Publisher, Dordrecht.

Regnier, P., A.W. Dale, S. Arndt, D.E. LaRowe, J. Mogollón, and P. Van Cappellen. 2011. Quantitative analysis of anaerobic oxidation of methane (AOM) in marine sediments: A modeling perspective. *Earth-Science Reviews* 106:105–130, http://dx.doi.org/10.1016/j.earscirev.2011.01.002.

Reznikov, A.A., E.P. Mulikovskaya, and I.Y. Sokolov. 1970. *Methods of Water Analysis,* 3rd ed. Moscow: Nedra, 488 pp. [in Russian]

Savvichev, A., I. Rusanov, G. Pavlova, T. Prusakova, V. Erochin, A. Lein, M. Ivanov, and K. Crane. 2004. Microbiological and biogeochemical explorations in Chukchi Sea (R/V *Professor Khromov*, July–August 2004). Slide presentation. http://www.arctic.noaa.gov/rusalca/sites/default/files/atoms/files/Microbiological and biogeochemical sampling Savvichev.pdf.

Savvichev, A.S., I.I. Rusanov, N.V. Pimenov, E.E. Zakharova, E.F. Veslopolova, A.Yu. Lein, K. Crane, and M.V. Ivanov. 2007. Microbial processes of the carbon and sulfur cycles in the Chukchi Sea. *Microbiology* 76(5):603–613, http://dx.doi.org/10.1134/S0026261707050141.

Schulz, S., and R. Conrad. 1996. Influence of temperature on pathways to methane production in the permanently cold profundal sediment of Lake Constance. *FEMS Microbiology Ecology* 20:1–14, http://dx.doi.org/10.1016/0168-6496(96)00009-8.

Schulz, S., H. Matsuyama, and R. Conrad. 1997. Temperature dependence of methane production from different precursors in a profundal sediment (Lake Constance). *FEMS Microbiology Ecology* 22:207–213, http://dx.doi.org/10.1111/j.1574-6941.1997.tb00372.x.

Shakhova, N., I. Semiletov, A. Salyuk, V. Yusupov, D. Kosmach, and Ö. Gustafsson. 2010. Extensive methane venting to the atmosphere from sediments of the East Siberian Arctic shelf. *Science* 327:1,246–1,250, http://dx.doi.org/10.1126/science.1182221.

State Geological Map of Russian Federation. 2006. Sheet S-1, 2 (The Chukchi Sea). Scale 1:1,000,000. *St. Petersburg. Map factory VSEGEI*. [in Russian]

Stein, R., K. Dittmers, K. Fahl, M. Kraus, J. Matthiessen, F. Niessen, M. Pirrung, Ye. Polyakova, F. Schoster, T. Steinke, and others. 2004. Arctic (palaeo) river discharge and environmental change: Evidence from the Holocene Kara Sea sedimentary record. *Quaternary Science Reviews* 23:1,485–1,511, http://dx.doi.org/10.1016/j.quascirev.2003.12.004.

Svitoch, A.A., and E.E. Taldenkova 1994. Recent history of the Bering Strait. *Oceanology* 34(3):439–443.

Thurston, D.K., and L.A. Theiss. 1987. *Geologic Report for the Chukchi Sea Planning Area, Alaska: Regional Geology, Petroleum Geology, and Environmental Geology*. OCS Report MMS 87-0046. US Department of the Interior, Minerals Management Service, Alaska OCS Region, Anchorage, Alaska, pp. 206.

Tolson, R.B. 1987. Structure and stratigraphy of the Hope Basin, southern Chukchi Sea, Alaska. 1987. Pp. 59–71 in *Geology and Resource Potential of the Continental Margin of Western North America and Adjacent Ocean Basins: Beaufort Sea to Baja California.* D.W. Scholl, A. Grantz, and J.G. Vedder, eds, Circum-Pacific Council for Energy and Mineral Resources, Earth Science Series, Houston, Texas.

Verzhbitsky, V., E. Frantzen, K. Trommestad, T. Savostina, A. Little, S.D. Sokolov, M.I. Tuchkova, T. Travis, O. Martyntsiva, and M. Ullnaess. 2008. New seismic data on the South and North Chukchi sedimentary basins and the Wrangel Arch and their significance for the geology of Chukchi Sea shelf. Abstract B030 in *Proceedings of the 3rd St. Petersburg International Conference and Exhibition on Geosciences – Geosciences: From New Ideas to New Discoveries*. April 7–10, 2008, Lenexpo, St. Petersburg, Russia.

Vinogradov, V.A., E.A. Gusev, and B.G. Lopatin. 2006. Structure of the Russian eastern Arctic shelf. Pp. 90–98 in *Proceedings of the Fourth International Conference on Arctic Margins ICAM IV*, September 30–October 3, 2003, Bedford Institute of Oceanography, Dartmouth, Nova Scotia, Canada.

Viscosi-Shirley, C. 2000. Siberian-Arctic Shelf surface-sediments sources, transport pathways and processes, and diagenetic alteration. PhD Dissertation, Oregon State University, Corvallis, OR.

Viscosi-Shirley, C., N. Pisias, and K. Mammone. 2003. Sediment source strength, transport pathways and accumulation patterns on the Siberian–Arctic's Chukchi and Laptev shelves. *Continental Shelf Research* 23:1,201–1,225, http://dx.doi.org/10.1016/S0278-4343(03)00090-6.

Wallmann, K., G. Aloisi, M. Haeckel, A. Obzhirov, G. Pavlova, and P. Tishchenko. 2006. Kinetics of organic matter degradation, microbial methane generation, and gas hydrate formation in anoxic marine sediments. *Geochimica et Cosmochimica Acta* 70:3,905–3,927, http://dx.doi.org/10.1016/j.gca.2006.06.003.

Wallmann, K., E. Pinero, E. Burwicz, M. Haeckel, C. Hensen, A. Dale, and L. Ruepke. 2012. The global inventory of methane hydrate in marine sediments: A theoretical approach. *Energies* 5:2,449–2,498, http://dx.doi.org/10.3390/en5072449.

Walsh, J.J. 1989. Arctic carbon sinks: Present and future. *Global Biogeochemical Cycles* 3:393–411, http://dx.doi.org/10.1029/GB003i004p00393.

Weingartner, T., K. Aagaard, R. Woodgate, S. Danielson, Y. Sasaki, and D. Cavalieri. 2005. Circulation on the north central Chukchi Sea Shelf. *Deep Sea Research Part II* 52:3,150–3,174, http://dx.doi.org/10.1016/j.dsr2.2005.10.015.

Yamamoto, S., J.B. Alcauskas, and T.E. Crozier. 1976. Solubility of methane in distilled water and seawater. *Journal of Chemical and Engineering Data* 21(1):78–80, http://dx.doi.org/10.1021/je60068a029.

Yashin, D.S., I.A. Andreeva, V.A. Kosheleva, and L.V. Polyak. 1985. *Structure, Material Structure and Geochemistry of Ground Adjournment of the Arctic Water Areas*. Report of the VNIIOkeangeologia, Leningrad, USSR, 237 pp. [in Russian]

Yashin, D.S., and B.I. Kim. 2007. Geochemical evidences of oil and gas content in Russian Eastern Arctic shelf. *Oil and Gas Geology* 4:25–29. [in Russian]

Yashin, D.S., O.V. Kirillov, A.P. Merkur'eva, L.V. Polyak, I.A. Alekseeva, and N.A. Pashukova. 1981. *Organic Substance and Hydrocarbonic Gases of Ground Deposits of the Arctic Seas USSR*. Report of the NIIGA, Leningrad, USSR, 215 pp. [in Russian]

Zeikus, J.G., and M.R. Winfrey. 1976. Temperature limitation of methanogenesis in aquatic sediments. *Applied and Environmental Microbiology* 31(1):99–107.

ACKNOWLEDGMENTS

We would like to thank the captain and crew of R/V *Professor Khromov*. Special thanks to Petr Semenov (VNIIOkeangeologia) and Eduard Prasolov from VSEGEI, who conducted molecular and isotopic measurements of hydrocarbon gases. We are also grateful to Nikolai Shchur (SPbPU) for great help with the modeling setup and Evgeny Gusev (VNIIOkeangeologia) for a fruitful discussion about sedimentological regimes and features of the Chukchi seafloor. We wish to thank referees Martin Hovland and Akihiro Hachikubo for their considered and thoughtful reviews of this paper, and we thank Kathleen Crane (Arctic Research Program, National Oceanic and Atmospheric Administration) for her support during the expeditions and preparation of the manuscript. We gratefully acknowledge SHELL HEFTEGAS DEVELOPMENT (V) LLC, which partly supported this study.

APPENDIX A. GEOCHEMICAL ANALYSIS TECHNIQUES

Geochemical analyses performed on pore waters, sediment, and water gases include major element, gas, and isotopic compositions. Major element geochemistry of pore water samples was determined in VNIIOkeangeologia using a method described by Reznikov et al. (1970). Cl^-, Ca^{2+}, and Mg^{2+} were determined by titration (argento-, acide-, and complexometry, respectively) The SO_4^{2-} species was determined by weight, and Na^+ and K^+ using flame photometry. Accuracy of the method is ± 0.01 mg L^{-1} for the K, Na, Mg, Ca, Cl, and SO_4 ions, and ± 0.1 mg L^{-1} for the HCO_3 and CO_2 ions. The sensitivity of the method depends on the volume of the measured water sample.

Wet sediments were transferred to gas-tight vials to determine the methane concentration using a routine head-space technique. Methane was measured in an onshore VNIIOkeangeologia lab using Shimadzu GC 2014 equipped with a flame ionization detector. A wide-bore capillary column Restek Aluminia (0.53 mm; 50 m) was employed to separate methane from other hydrocarbon gases. The carrier gas was He flowing at a rate of 20 mL min^{-1}. Peaks were calibrated against certified standard gas mixtures.

The organic carbon content (C_{org}) (i.e., oxidizable organic carbon) was determined by using the "wet" (dichromate) method of carbon combustion using AN-7529 automatic carbon analyzer. The percent organic carbon (C_{org}) was calculated by the difference: (C_{org} = total C – inorganic C).

Sulfate reduction rates were measured by tracing isotopically labeled sulfate in incubated sediments. The sulfate reduction rate was determined by the formation of ^{35}S-labeled H_2S, total pyrite, and elemental and organic sulfur from $Na_2{}^{35}SO_4$ (0.2 ml, 35 µCi per 5 cm^3 of the sediment). The samples were treated according to the procedures described in Gal'chenko (1994).

The anaerobic oxidation of methane (AOM), sulfate reduction (SR), and methanogenesis (MG) rates were determined using measurements of sedimentary CH_4, pore water sulfate (SO_4^{2-}), and organic matter content (C_{org}) at two study sites combined with simulations of the methane cycle transport-reaction processes. Modeled sulfate reduction rates were compared and validated by the rates determined by ^{35}S tracer experiments carried out in this study. Modeled AOM and MG rates were compared with measured data on

closely located RUSALCA coring stations reported in Savvichev et al. (2007).

Measurements of isotope compositions of methane carbon ($\delta^{13}C(CH_4)$) were carried out at the Centre of Isotopic Research of VSEGEI (St. Petersburg) using an isotope-ratio-monitoring mass spectrometric (IRM–MS) method by means of a DELTA plus XL mass spectrometer with a GC/C-III device (ThermoFinnigan production) for the gas measurements. Random error during the determination of carbon isotopic composition (1σ) was in the range of 0.1–0.2‰. The results of isotopic measurements are represented in per-mil delta notations (‰) relative to PDB standard.

APPENDIX B. NUMERICAL TRANSPORT-REACTION MODEL SETUP

The model calculates the concentration-depth profiles of two dissolved species—sulfate and methane. Partial differential equations were set up following the classical approach used in early diagenesis modeling:

$$\frac{\partial ci(z,t)}{\partial t} = \frac{\partial}{\partial z}\left(Ds \cdot \frac{\partial ci(z,t)}{\partial z}\right) - \frac{\partial(\varphi(z,t) \cdot u(z) \cdot ci(z,t))}{\partial z} + \varphi(z,t) \cdot \Sigma Rd(z,t) \quad (1)$$

where ∑Rd (mol/cm^3·s) is the sum of rates of all considered reactions; ci is the concentration of species i in the liquid (moles per fluid volume, mol m^{-3}). On the left side of Equation (1) are terms corresponding to accumulation of species mass within the liquid phase. On the right side, the first term introduces diffusion; the second term describes the convection due to the directional velocity, and the last term describes production or consumption of the species. The system of differential equations was solved using Comsol Multiphysics. Conditions approaching steady state for solute concentrations are attained in about 15,000 years of simulation time for HC-10 and 100,000 years for HC-4.

Initial and Boundary Conditions. Initial conditions for methane throughout the column were designated as 0 mM, and for sulfate, the value measured in the pore water from surficial sediment (Figure 3B). The lower boundary conditions for methane were assumed to be based on a no-flux boundary for station HC-10, assuming bacterial methane generation via organic matter degradation. Taking into account the migration origin of methane according to its molecular composition, low Bernard ratio, and interpretations of the seismic data, we set the methane flux and sulfate concentration at the base of the modeled domain in core HC-4 and the upper methane boundary at zero for both sites. The minimum domain length is calculated according to Mogollón et al. (2012). The lower boundary was placed at a depth greater than the diffusive length scale of Holocene sediment ($L > \sqrt{4Dm \cdot T}$), where Dm is the molecular diffusion coefficient for methane, T = 11,700 yr), that is at L > 34.6 m. Thus, the thickness of the modeled domain is 35 m in both simulations.

APPENDIX C. KINETICS OF ORGANIC MATTER DEGRADATION

To estimate the amount of particulate organic carbon (POC) that could reach the methanogenesis zone and be further converted to methane, we need know the POC burial rates and downcore changes in POC reactivity, which decreases strongly with sediment age and depth. A synthesis of the Middelburg (1989) classic organic matter degradation model, as modified by Wallmann et al. (2006), predicts that organic matter degradation rates are not affected by pore water composition but are suppressed by the accumulation of dissolved metabolites. The improved Wallmann et al. (2006) model describes the effect of metabolite concentrations on anaerobic POC degradation in anoxic marine sediments by the equation

$$R_{OMD} = \frac{K_c}{(C_{DIC} + C_{CH4} + K_c)} \cdot k_{OMD} \cdot C_{CH2O} \quad (2)$$

where R_{OMD} is the organic matter degradation rate, $C_{(DIC)}$ is the concentration of dissolved inorganic carbon (CO_3 +HCO_3 +CO_2), $C_{(CH4)}$ is the methane concentration, k_{OMD} is an age-dependent kinetic constant, $C_{(CH2O)}$ is the organic matter concentration, and K_C is a Monod constant describing the inhibition of organic matter (OM) degradation by dissolved inorganic carbon (DIC) and CH_4. The rate law predicts that the microbial degradation of OM is inhibited by metabolites accumulating in adjacent pore fluids because the Gibb's free energy available for the microbial metabolism is reduced in the presence of high concentrations of reaction products.

The main uncertainty of the Middleburg model was associated with the initial age parameter (a_0), defined as the average age of POC buried below the bioturbation zone (Wallmann et al., 2006, 2012). According to Wallmann et al. (2012), the value of this parameter depends on ambient variability in burial velocity, the deposition of refractory organic matter, and the possible loss of surface sediments during core retrieval. With the absence of a complete data set necessary for the modeling, a_0 was determined by the best fit between the data and the model. The best fit was obtained at zero a_0 in the sediment core HC-10, indicating fast decay of the reactive pools. Indeed, the sediment in core HC-10 was highly reduced downcore and was characterized by a strong decreasing trend in the organic carbon values supporting the modeling results. For HC-4 the best fit to the measured sulfate and methane values was obtained at a_0 value of 30,000 years (see Table 1 and Figures 3 and 4).

AUTHORS

Tatiana Matveeva (tv_matveeva@mail.ru) is Academic Secretary-Head of Laboratory for Unconventional Hydrocarbon Resources, I.S. Gramberg VNIIOkeangeologia, St. Petersburg, Russia. **Alexander S. Savvichev** is Head of Laboratory for Microbiology and Biogeochemistry of Reservoirs, Winogradsky Institute of Microbiology, Russian Academy of Sciences, Moscow, Russia. **Anastasiia Semenova** is a researcher at the I.S. Gramberg VNIIOkeangeologia, St. Petersburg, Russia. **Elizaveta Logvina** is Senior Scientist, I.S. Gramberg VNIIOkeangeologia, St. Petersburg, Russia. **Alexander N. Kolesnik** is a researcher at the V.I. Il'ichev Pacific Oceanological Institute, Vladivostok, Russia. **Alexander A. Bosin** is a researcher at the V.I. Il'ichev Pacific Oceanological Institute, Vladivostok, Russia.

ARTICLE CITATION

Matveeva, T., A.S. Savvichev, A. Semenova, E. Logvina, A.N. Kolesnik, and A.A. Bosin. 2015. Source, origin, and spatial distribution of shallow sediment methane in the Chukchi Sea. *Oceanography* 28(3):202–217, http://dx.doi.org/10.5670/oceanog.2015.66.